Design Considerations For Remote High-Speed Pressure Measurements Of Dynamic Combustion Phenomena

Douglas L. Straub, Donald H. Ferguson
U.S. Department of Energy – National Energy Technology Laboratory, Morgantown, WV, 26505, USA

Robert Rohrssen and Eduardo Perez
West Virginia University, Morgantown, WV 26505, USA

As gas turbine combustion systems evolve to achieve ultra-low emission targets, monitoring and controlling dynamic combustion processes becomes increasingly important. These dynamic processes may include flame extinction, combustion-driven instabilities, or other dynamic combustion phenomena. Pressure sensors can be incorporated into the combustor liner design, but this approach is complicated by the harsh operating environment. One practical solution involves locating the sensor in a more remote location, such as outside the pressure casing. The sensor can be connected to the measurement point by small diameter tubing. Although this is a practical approach, the dynamics of the tubing can introduce significant errors into the pressure measurement. This paper addresses measurement errors associated with semi-infinite coil remote sensing setups and proposes an approach to improve the accuracy of these types of measurements.

Nomenclature

A	=	Cross-sectional area
c	=	Speed of sound
d	=	Diameter
J_0, J_1	=	Bessel Functions
L	=	Length
p	=	Acoustic pressure
Q	=	Reflection coefficient for a volume terminated line
R	=	Radius
V	=	Volume of pressure transducer cavity
W	=	Wave Shear Number
y	=	Propagation constant
Fr	=	Froude Friction Factor
Pr	=	Prandtl Number
α	=	Attenuation coefficient
γ	=	Ratio of specific heats
ρ	=	Density
ζ	=	Specific acoustic impedance
υ	=	Kinematic viscosity
ω	=	Angular frequency (rad/s)
Subscripts		
0, 1, 2	=	Reference stations for P_0, P_1, and P_2 (see Fig. 1 and Fig. 6)
e	=	Reference to the closed end of semi-infinite coil

I. Introduction

As gas turbine combustion systems evolve to lower pollutant emission targets, accurate measurements of dynamic combustion processes becomes increasingly important. The current goals of the U.S. Department of Energy's Turbine Program include NOx emissions of 2 parts-per-million and fuel-flexible requirements that may include hydrogen fuels produced from coal. Combustion dynamics, lean flame extinction, and flashback are some examples of combustion challenges that require high bandwidth sensors.

Typically, high-speed pressure transducers are the instrument of choice for monitoring dynamic combustion phenomena. High-speed pressure transducers have been used to monitor combustion-driven instabilities[1,2,3]; to predict the onset of combustion instabilities[4]; and to provide feedback for active control of combustion instabilities[5]. Pressure sensors have also been used to predict the onset of lean flame extinction[6] and even changes in flame anchoring.[7] In most gas turbine applications, these high speed pressure transducers are located a significant distance from the combustion chamber[1,8]. These remote sensing systems are typically used to avoid placing the sensor in the high temperature and high pressure environment near the combustion liner. In most cases, the pressure sensing system includes a mechanism (i.e., a waveguide or semi-infinite coil) to dampen acoustic reflections over the frequency range of interest. Generally speaking, the media in these waveguides are stationary (i.e., no mean flow) and the tubing diameters are small. As a result, the most important mechanisms for sound attenuation are due to the effects of viscosity and heat loss, otherwise known as visco-thermal effects.

The transfer function between the measured pressure and the actual combustor pressure can be predicted using theoretical expressions that are based on unsteady one-dimensional relations. These models can account for the geometry of the interconnecting hardware, the temperature gradients along the hardware[9] and visco-thermal losses[8]. However, Munjal[10] has shown that experimental measurements by several investigators can disagree with theoretical values by 15 to 50 percent. Additional measurements of attenuation performed by Ferrara et. al[11] for remote pressure sensing systems similar to those used in gas turbine applications indicate that in addition to the large uncertainty, the attenuation does not vary monotonically with frequency as theory suggests. It is interesting to note that the disagreement observed by Ferrara et. al[11] is of the same order as described by Munjal[10].

A. Background

Although the results of Ferrara et. al[11] were very applicable to the pressure sensing systems used in gas turbine applications, the errors associated with remote pressure measurements were not addressed. Furthermore, experimental evidence relative to these remote pressure sensing systems is difficult to find in the open literature.

Van Ommen et. al[12] describe theoretical and experimental results from a pressure sensing system for gas-solid fluidized bed applications in which the frequencies of interest are less than 200 Hertz. Although the pressure sensing system used in this work is not identical to the systems employed in gas turbine applications, Van Ommen et. al[12] show that even the best model (i.e., Bergh and Tijdeman[13] model) produces significant differences when compared to a reference probe placed in the fluidized bed. Although attenuation terms were included in the models, the potential error associated with these terms was not discussed and the authors attributed the errors to differences in the source location..

Mahan and Karchmer[14] provide a good discussion of the semi-infinite coil measurement technique with particular emphasis on gas turbine applications. The various sources of error, including a brief description regarding viscous attenuation are discussed. These authors note the dependence of viscous attenuation error on the experimental setup and recommend approaches to minimize these effects such as using shorter probes with larger diameters. However, no experimental data is provided.

Englund and Richards[15] discuss the key characteristics of designing a semi-infinite line pressure probe. However, the overall line lengths used in this study were relative short with the baseline probe design having a line length of two meters and the longest tube length being four meters. Furthermore, this work does not provide experimental verification of the transfer functions described.

In 1967, Samuelson[16] published a report that described remote pressure sensing for nuclear rocket engine testing. This report is probably the best review of the assumptions and limitations of the theory. The author provides some experimental data that shows good agreement with the theoretical models, but the frequency range of interest was less than 10 Hertz. According to Samuelson[16], Bergh and Tijdeman[13] have also shown that their segmented-line equation agrees with measured values to within 2–5 percent for a frequency range from 10-200 Hertz. Experimental data for frequencies above 200 Hertz could not be found in the open literature. Interestingly, the direct measurements of attenuation reported by Ferrara[11] suggest that discrepancies in the measured attenuation become significant for frequencies above 150 Hertz. Since most combustion instabilities occur at frequencies higher than

150 Hertz, it is important to understand the pressure measurement implications as a result of uncertainties in the attenuation factors.

B. Scope

In the ideal situation, the pressure transducer could be placed directly into the combustion environment and the errors introduced by the waveguide, or semi-infinite coil, could be avoided. However, this approach is limited by the maximum service temperature of the pressure transducer. Therefore, it is sometimes necessary to attach the pressure transducer to a remote sensing unit, such as a semi-infinite coil. Based on information available in the literature[1], a continuous gas purge is not a common practice for remote sensing units used on most gas turbine systems, and as a result the attenuation in these systems is primarily due to visco-thermal effects.

This paper will focus on the semi-infinite coil approach with no purge gas, or mean flow, through the remote pressure sensing unit. Utilizing experimental data obtained through this study, theoretically derived transfer functions relating the pressure measured in the remote unit to the desired pressure in the main body of a simulated gas turbine combustor are compared to the actual measured response. Since viscous attenuation is sensitive to surface imperfections and several other apparatus specific conditions, the data presented in this paper is specific to this experimental setup. However, these results may provide an order of magnitude estimate of the errors for remote pressure sensor configurations that incorporate a semi-infinite coil arrangement.

II. Experimental Setup

Figure 1 shows a sketch of the experimental closed-opened tube arrangement used to simulate a gas turbine combustor. A 43 cm (17 in) long, 7.6 cm (3 in) diameter commercial plastic (PVC) pipe is attached to a speaker enclosure on one end while the other end is open to the room. The remaining system components consist of a speaker (Boston Model G212), an amplifier (Realistic Model 32-2027A), and a spectrum analyzer/frequency generator (Agilent Model 35670A). Pressure s ır (P_0) and in the remote sensing unit (P_1). The sensor at station P_0 is flush-mounted in the walls of the pipe while the sensor at station P_1 is inserted into a block that orients the sensor normal to the tube wall and minimizes the volume of the transducer cavity. The volume of the transducer cavity is approximately 0.1 cm^3 which is roughly three orders of magnitude smaller than the total volume of the tubing. The inside diameter of the interconnecting tubing for the semi-infinite coil is 3.8 mm (0.15-in) and the overall length of the remote sensing unit is approximately 12.93 meters (509 in). The coil arrangement allows for the distance between P_0 and P_1 to be varied.

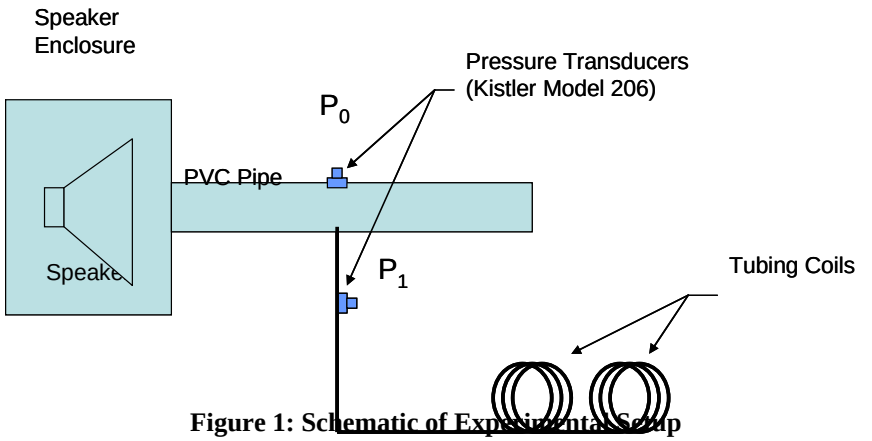

Figure 1: Schematic of Experimental Setup

The amplifier/speaker is excited using a random noise generator from the dynamic signal analyzer (Agilent 35670A). This analyzer is also used to compute the complex frequency response functions and the respective coherence functions. These functions are obtained from 150 spectral averages and the results are stored for post-processing in a MathCad program. Utilizing the coherence as a filter, data with values less than 0.98 have been rejected.

III. Data Analysis

A. Segmented Line Equation Model (Bergh and Tijdeman[13])

This model is an extension of the work of Iberall[17] (1950) and is considered by others[12,16] to be the best approach for this type of problem. Samuelson[16] provides a good overview of the assumptions required to simplify Bergh and Tijdeman's generalized segmented-line equation into the expression shown in Eq. 1. The key assumption is that the tubing is homogeneous everywhere, except at the transducer tap.

$$\frac{P_1}{P_0}(i\omega) = \left[\cosh(yL_{01}) + Q\sinh(yL_{01}) + \left(\sinh(yL_{01})\tanh(yL_{1e})\right)\right]^{-1} \tag{1}$$

The volume of the transducer cavity, V, is incorporated into the reflection coefficient, Q. According to Samuelson[16], the reflection coefficient for an adiabatic expansion in the transducer cavity can be expressed as shown in Eq. 2. Zero and first order Bessel Functions are denoted by J_0 and J_1, respectively. The arguments for the Bessel Functions are the dimensionless shear wave number, W, (see Eq. 3) and the product of the shear number and the Prandtl Number, E (see Eq. 4). Note that the value of Q becomes more significant as product of the transducer volume and the frequency increases given a constant cross-sectional area of the interconnecting tubing, A, and speed of sound, c.

$$Q = \frac{\omega V}{cA}\left[\frac{1}{\left[1+\frac{2(\gamma-1)\cdot J_1(E)}{E\cdot J_0(E)}\right]\cdot\left[\frac{2\cdot J_1(W)}{W\cdot J_0(W)}-1\right]}\right]^{\frac{1}{2}} \tag{2}$$

$$W^2 = R^2\cdot\left(\frac{-i\omega\rho}{\mu}\right) = R^2\left(-\frac{i\omega}{\nu}\right) \tag{3}$$

$$E = \Pr\cdot W \tag{4}$$

The second parameter in Eq. 1 that must be defined is the propagation constant, y (see Eq. 5). Although Samuelson[16] describes simplifications to these expressions depending on the range of shear numbers expected in the problem, none of these simplifications will be used in the analysis presented below.

$$y = \frac{\omega}{c}\cdot\left[\frac{1+\frac{2(\gamma-1)\cdot J_1(E)}{E\cdot J_0(E)}}{\frac{2\cdot J_1(W)}{W\cdot J_0(W)}-1}\right]^{\frac{1}{2}} \tag{5}$$

It should be noted that the term in square brackets represents the attenuation due to visco-thermal effects. This attenuation term is composed of an imaginary and a real component. The imaginary component is sometimes called the phase-shift coefficient, and the real component is called the attenuation coefficient. This will be described in more detail in the next section.

B. Viscous Attenuation Terms

As previously mentioned, viscosity and heat loss effects are the primary attenuation mechanisms for sound waves propagating through small diameter tubes containing a stationary media. It is interesting to note that these visco-thermal loss coefficients are not always reported consistently in introductory acoustic textbooks. For example, Munjal[10] and Kinsler[18] have slightly different expressions for the visco-thermal attenuation coefficient and both of these expressions differ from the attenuation coefficient (the real component of the term in the square brackets) of Eq. 5. Figure 2 shows a comparison between the attenuation coefficients from Munjal[10], Kinsler[18], and Samuelson[16]. Note that the expressions from Munjal[10] and Kinsler[18] have been normalized by the wave number (i.e., ω/c) to express them in dimensionless form. All three expressions agree for large shear wave numbers (i.e. W>30) where viscous damping is very low. However, for the experimental setup described in this paper, the frequency range of interest is 100-800 Hertz and the corresponding shear wave numbers are in the range of 10-30. Therefore, Eq. 5 will be used.

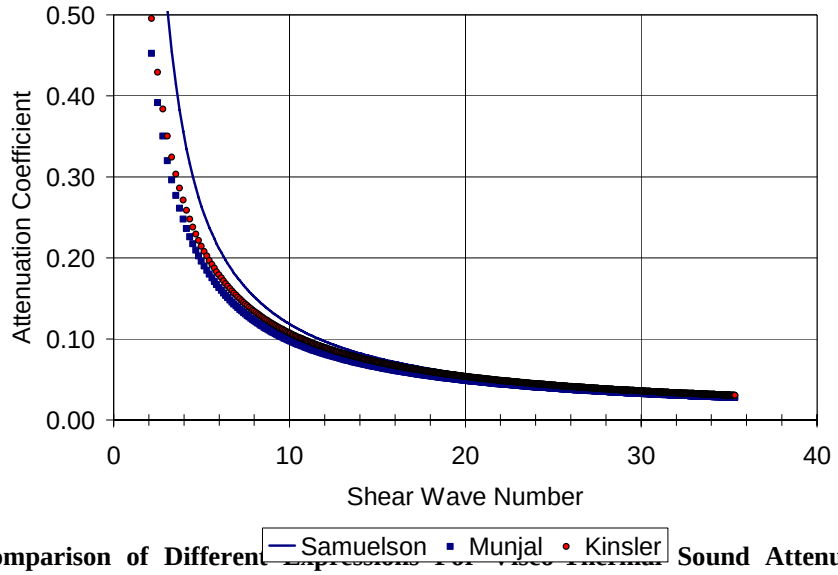

Figure 2: Comparison of Different Expressions For Wave Thermal Sound Attenuation in Tubes with Circular Cross-Section

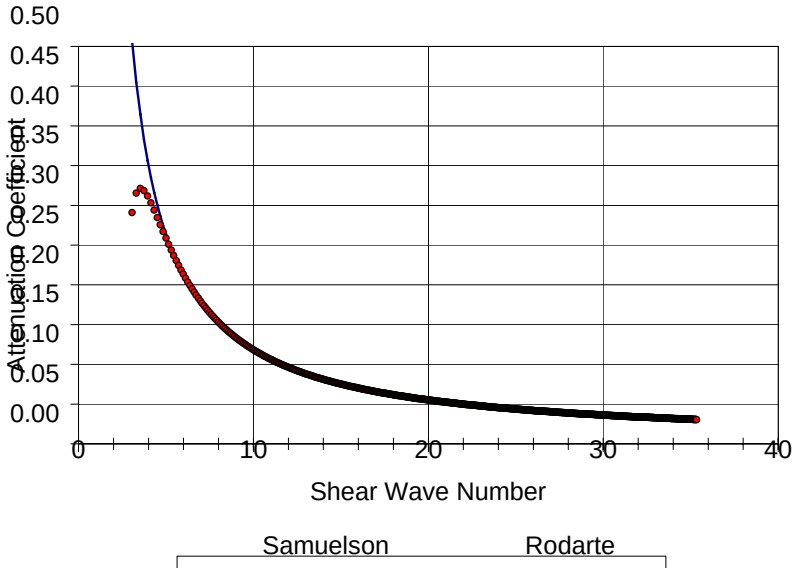

Figure 3: Comparison of Attenuation Coefficient With Bessel Functions To Curve-Fit Developed By Rodarte et. al[19]

It is interesting to note that a polynomial fit for the attenuation coefficient has been developed by Rodarte et. al[19]. This curve fit is applicable for a wide range of gases and does not involve Bessel Functions. Figure 3 shows a comparison between Rodarte's curve-fit and the attenuation coefficient that can be obtained from Eq. 5. Note that the curve-fit begins to deviate for shear wave numbers less than about six. For the configuration studied in this paper, this corresponds to frequencies of less than 10 Hertz which was outside the low frequency cutoff for the speaker.

IV. Discussion of Results

A. Segmented-Line Model

Figure 4 shows the frequency response data collected from pressure sensor P_1 located approximately 54.6 cm (21.5 in) away from the desired measurement plane, P_0. A semi-infinite coil that is approximately 12.2 m (40 ft) long is used to dampen the pressure waves that propagate past P_1. The interconnecting tubing has a 3.8 mm (0.15 in) inside diameter, and the media is air at atmospheric pressure and ambient temperature. The predicted response utilizes the model described in Equations 1-5 to calculate a relationship between the desired pressure and the measured pressure in the remote sensing unit. As shown in Fig. 4, the measured and predicted gains show some fairly significant discrepancies. The discrepancies in the low frequency range from 2-15 percent for frequencies below 100 Hz, and the discrepancy becomes larger at higher frequencies. It should be noted that the larger discrepancies near 150 Hz may be due to some systematic errors associated with dynamic interactions with the speaker enclosure. Therefore, although the data shown has a coherence of greater than 0.98, due to the interactions with the speaker enclosure, the gain data in the 150 Hz range may be somewhat biased.

At high frequency, the measured gain is considerably more complex than the model suggests. It should be noted that the non-linearity in the model gain (solid line in Fig. 4) is due to the volume of the transducer cavity. If the volume (i.e., Q parameter) is neglected in Eq. 1, the predicted gain decreases monotonically for these higher

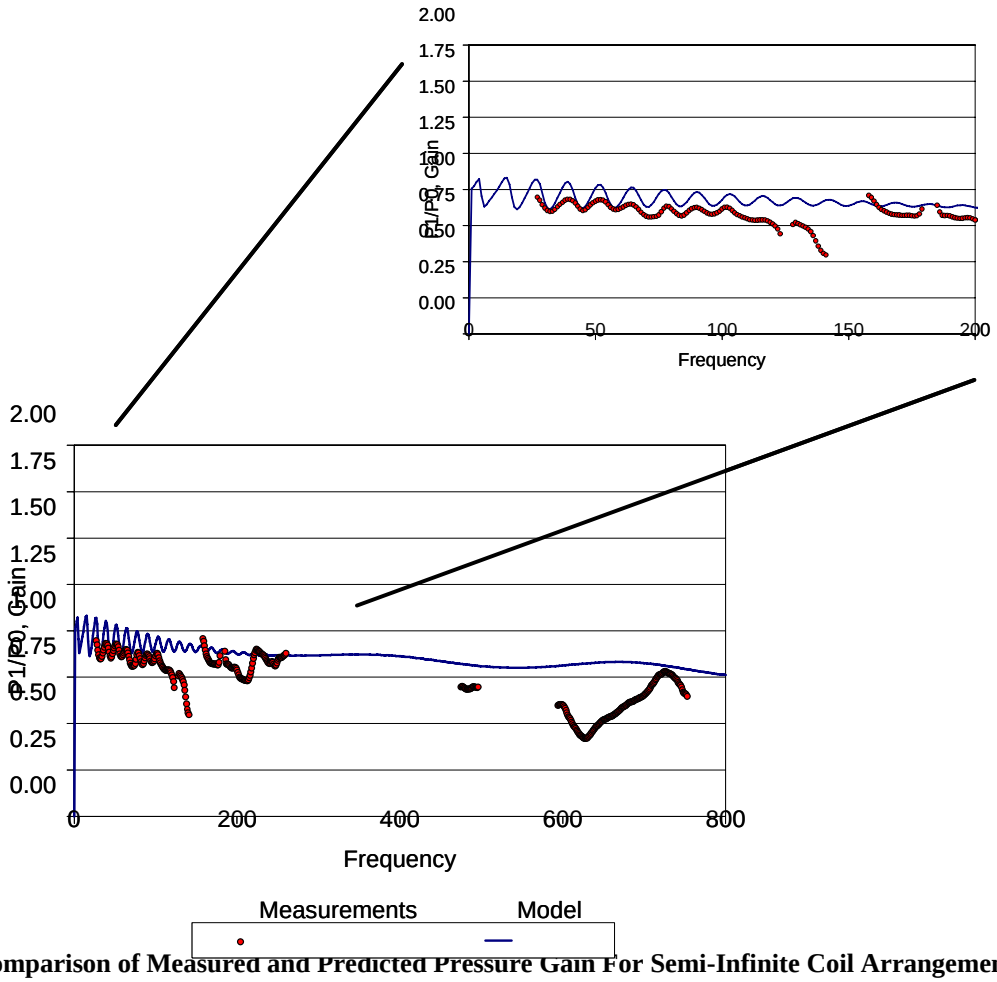

Figure 4: Comparison of Measured and Predicted Pressure Gain For Semi-Infinite Coil Arrangement

frequencies. In addition to the significant differences observed between the measured and calculated gains for the pressure transfer function, it is not clear that the qualitative features of the measured gain can be recovered using the model approach described here. It is interesting to note that the model predictions of gain are significantly higher which suggests that the attenuation is under-predicted by the model. This is consistent with the attenuation measurements of Ferrara et. al[11]. Likewise, Ferrara et. al[11] observed that measured values of the attenuation do not vary monotonically as theory suggests, particularly at higher frequencies.

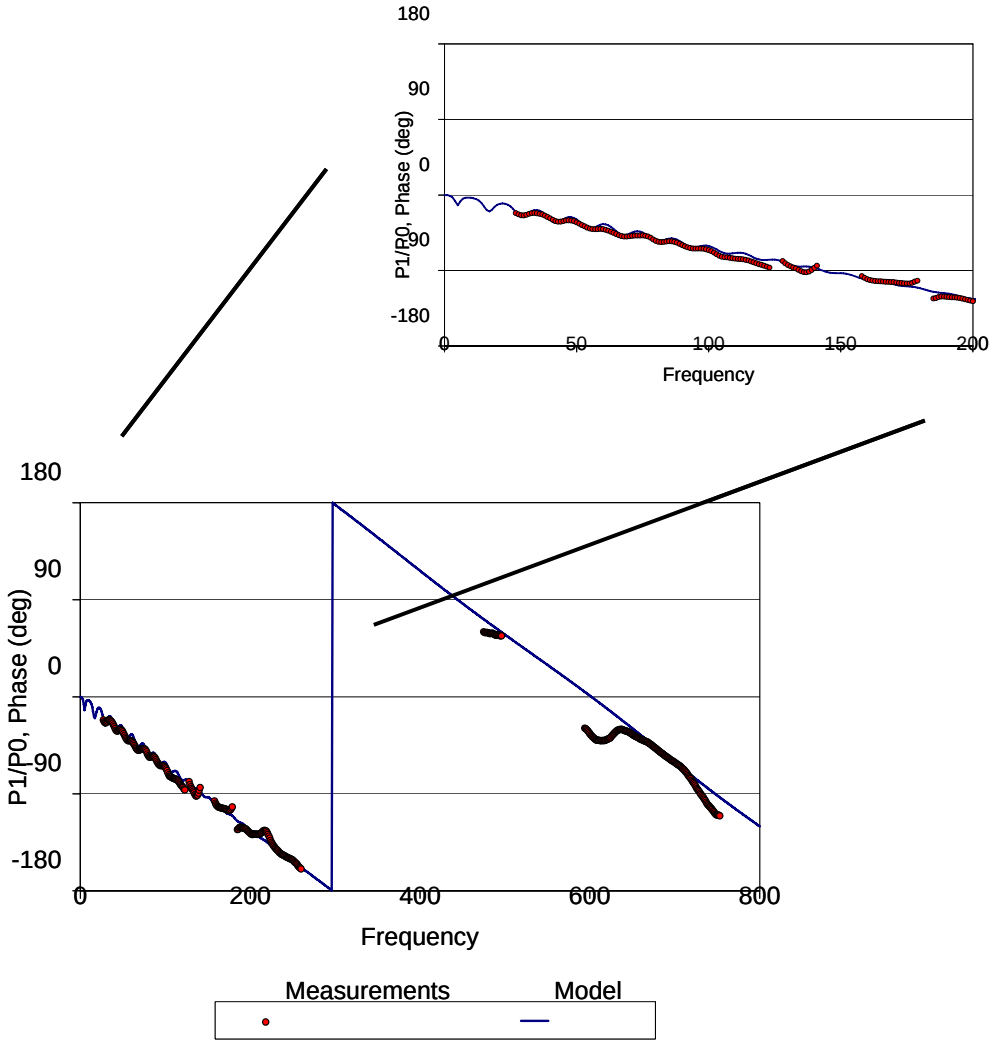

Figure 5: Comparison of Measured and Predicted Phase Angles For Pressure Measurements in a Semi-Infinite Coil Arrangement

Figure 5 shows the phase angle measurements and model predictions for a frequency range of 50-750 Hz. At low frequencies (i.e. less than 200 Hz), the agreement between the measured and predicted phase angle is very good. Even the local minima and maxima in the low frequency response can be predicted within 10 degrees of the measured phase angle (see inset of Fig. 5). At higher frequencies, however, the measured and predicted phase angles show larger differences (i.e., 20-40 degree differences) at some frequencies. Furthermore, the measured phase angles do not decrease monotonically with frequency.

B. Two-Sensor Segmented-Line Model

In an attempt to improve the model predictions, a slightly different approach has been taken as shown in Fig. 6. In this approach, two pressure sensors are placed in the semi-infinite coil arrangement. By using the measured frequency response between these two sensors, acoustic properties (i.e., pressure, velocity, impedance, etc.) can be

calculated at other locations in the system (Munjal[10]). This technique is widely used and is commonly known as a two-microphone approach. The experimental setup is nearly identical, except that a short (15.2 cm) length of tubing has been removed and replaced with a second pressure transducer block. The spacing between these two sensors is 15.2 cm (6 in).

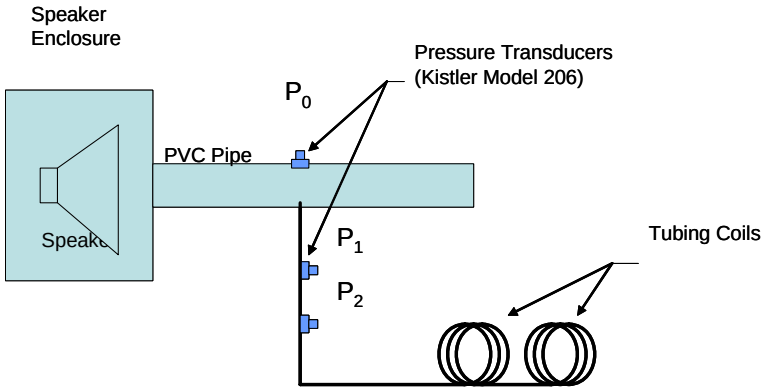

Figure 6: Modified Two-Sensor Approach Using a Semi-Infinite Waveguide

measured frequency response between P_1 and P_2. This is a fairly straightforward application of the segmented-line equations developed by Bergh and Tijdeman[13] and summarized by Samuelson[16] (see Eq. 6). Note that the term associated with the semi-infinite wave guide (i.e., L_{1e}, the coil length) no longer has an effect on the predicted transfer function between P_1 and P_0. Instead, this term is replaced with the measured frequency response between P_2 and P_1.

$$\frac{P_1}{P_0}(i\omega) = \left[\cosh(yL_{01}) + Q\sinh(yL_{01}) + \frac{\sinh(yL_{01})}{\sinh(yL_{12})}\cdot\left(\cosh(yL_{12}) - \frac{P_2}{P_1}(i\omega)\right)\right]^{-1} \tag{6}$$

Figure 7 shows the measured and predicted gain using Eq. 6. Note that the low frequency data (i.e., less than 200 Hz) is shown in the inset. The discrepancies between the measured gain and the predicted gain are still significant at certain frequencies. However, the complex behavior of the high frequency gain is improved by combining the theory and the second pressure sensor measurement. Contrary to the previous approach, the calculated gain is under-predicted at the highest frequency range. Although this two-sensor approach is capable of reproducing some of the qualitative features of the high frequency gain, more work is required to improve the accuracy of these measurements.

Figure 8 shows the measured and predicted phase angles using Eq. 6. Once again, the measured and predicted phase angles agree reasonably well, over the entire frequency range. However, it is important to note that the measured phase angles at high frequency are slightly different than the phase angles measured with the single sensor arrangement (see Fig. 5). This difference may be due to the fact that these two configurations are physically different and the presence of the second transducer volume (P_2) could change the dynamic response of the system, particularly at high frequencies.

V. Summary

Dynamic pressure measurements are a popular choice to monitor dynamic combustion phenomena in some gas turbine applications. Due to the harsh environment around the combustion liner, the pressure transducer is often located a significant distance away from the measurement point of interest. The interconnecting tubing between the combustion liner and the pressure transducer is comprised of small diameter tubing and the media within the tubing is stationary. As a result, visco-thermal attenuation of the pressure waves in the interconnecting tubing can be significant. Theoretical transfer functions attempt to account for this attenuation, but according to other studies[10,11] textbook expressions for the visco-thermal attenuation show significant disagreement with experimental measurements.

Given the uncertainties in the visco-thermal attenuation terms, errors can be expected for pressure measurements using a semi-infinite waveguide. These errors can have implications for monitoring combustion dynamics and

active control systems which use high speed pressure sensors for feedback control. Previous efforts[12,15,16,19] have investigated the semi-infinite wave-guide approach and found that the segmented-line equation developed by Berg and Tijdeman[13] is the best approach for predicting wave propagation through small diameter tubes with no mean flow. However, experimental data to validate the segmented-line model of Berg and Tijdeman is limited to frequencies below 200 Hertz. Since the frequency range of interest for most gas turbine combustion phenomena is higher than 200 Hertz, this paper provides some experimental data on the semi-infinite coil approach and compares these measurements to the model results. The segmented-line equation is modified slightly to include a second sensor in the semi-infinite coil to improve the accuracy at high frequency conditions.

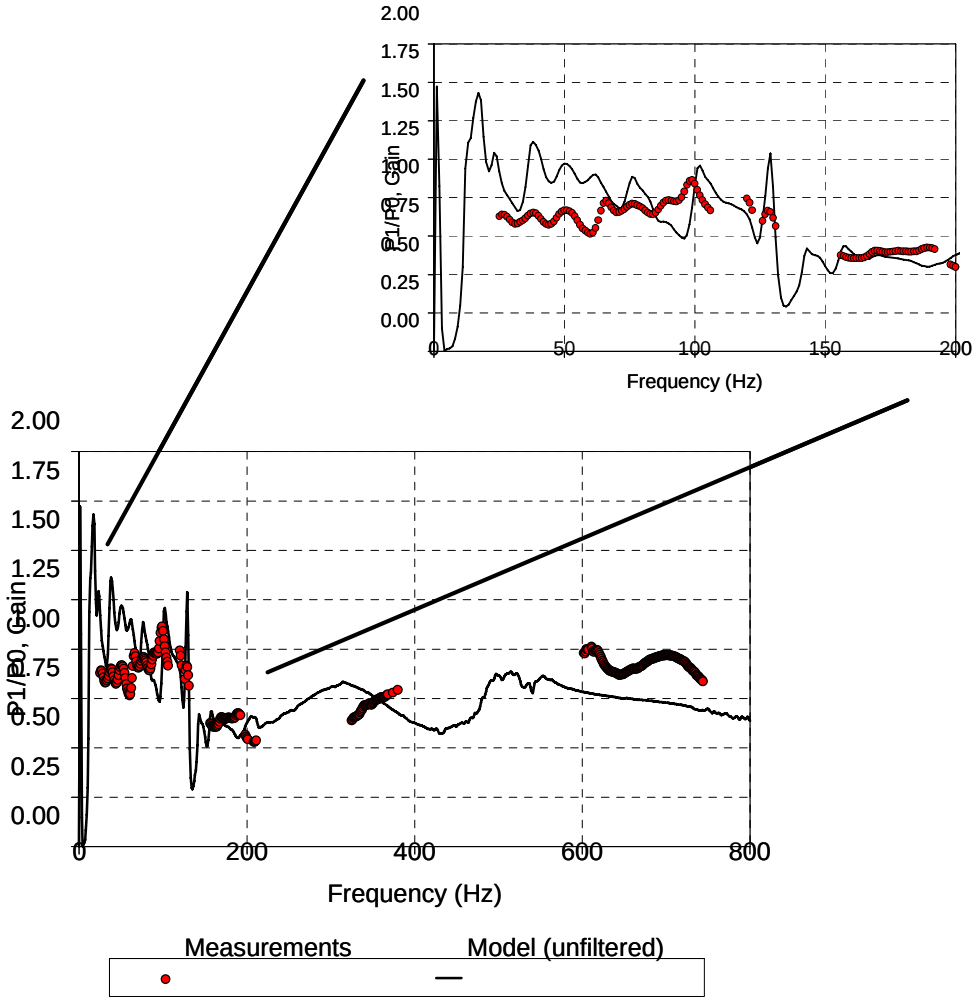

Figure 7: Comparison of Gain Measurements with Model Using Two-Sensor Segmented Line Equation

VI. Conclusions

For the single sensor arrangement studied in this paper, the segmented line approach predicted transfer function gain values that are within 2-15% of the measured values for frequencies below 100 Hz. For the two sensor approach, the errors in the gain predictions range from 10-50 percent for these low frequencies. At higher frequencies (i.e., 600-800 Hz), discrepancies of 80-90% have been observed with the predicting the gain using a single sensor approach, whereas discrepancies on the order of 20 percent are observed for the two sensor approach. It should be noted that the data between 250 Hz and 600 Hz was sparse due to low coherence in this region.

For the single sensor arrangement, the predicted phase angles agree to within 15 degrees over the entire frequency range of 30-750 Hz. For the two sensor arrangement, the predicted phase angles agree to within 20-30 degrees for all frequencies. It should be noted that the two sensor approach provides more accurate predictions of the phase angle behavior at high frequencies, whereas, the single sensor approach provides better predictions in the low frequency range.

High-speed pressure measurements of dynamic combustion phenomena are not trivial. These types of pressure measurements become increasingly complex when a frequency response of higher than 150-200 Hertz is required for a remote sensing unit such as a semi-infinite coil apparatus. In order to simplify the theoretical analysis, it is imperative to maintain a homogenous cross-section. Any changes in the internal cross-sectional area or the presence of a side-branch volume will change the high frequency response of the system.

For the experimental setup described in this paper, the discrepancies between the measured and calculated transfer functions are significant for applications, such as active feedback control of combustion instabilities. It is believed that much of the discrepancy may be due to the theoretical estimates of visco-thermal attenuation. The two-sensor approach described here may help improve the high frequency predictions, but there is still room for improving these types of high-bandwidth pressure measurements.

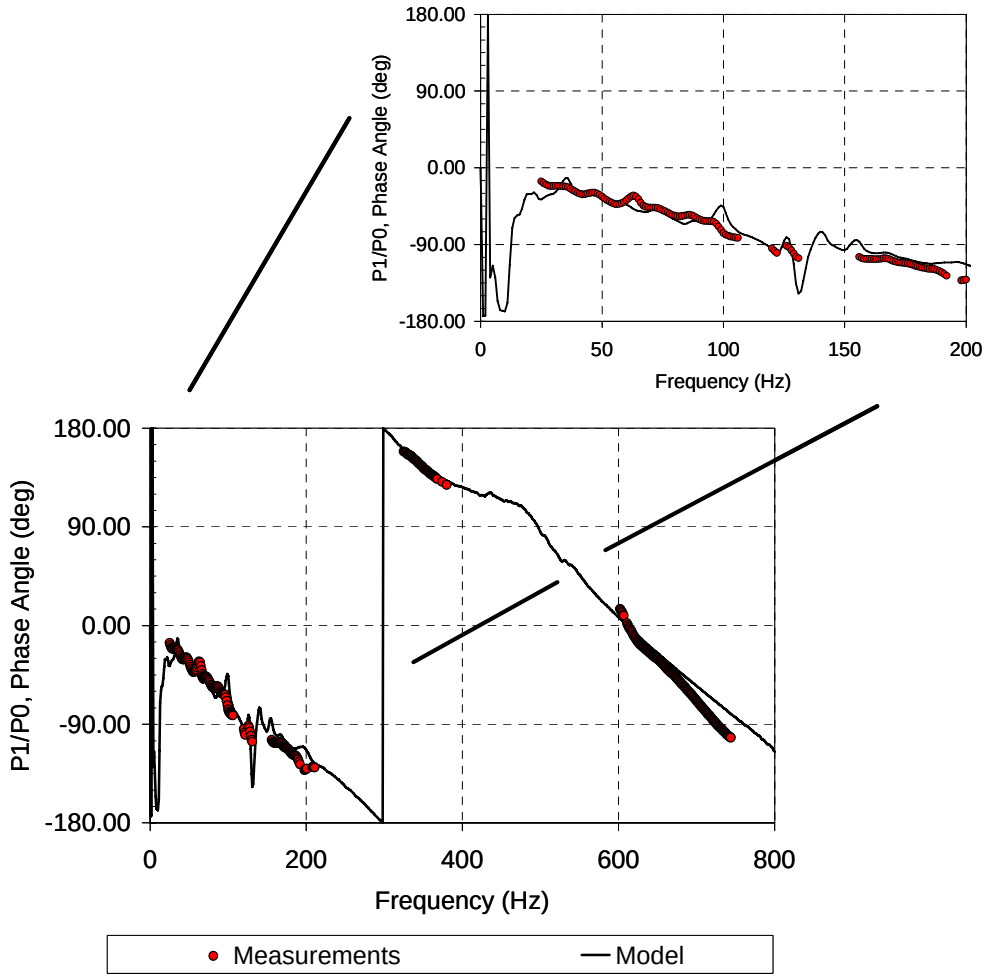

Figure 8: Comparison of Phase Angle Measurements with Model Using Two-Sensor Segmented Line Equation

VII. Acknowledgements

The authors gratefully acknowledge the support of the DOE Fossil Energy Turbines Program and Mr. Richard Dennis, the Technology Manager for the Turbines Program. Robert Rohrssen acknowledges the support of the Oak Ridge Institute of Science and Engineering (ORISE) Professional Internship program. The authors also acknowledge the gracious advice from Dr. Geo. Richards and Dr. Eric Johnson.

VIII. References

[1] ~~Lieuwen, T. C. and Yang, V. (ed~~.), "Combustion Instabilities in Gas Turbine Engines: Operational Experience, Fundamental Mechanisms, and Modeling," *Progress in Astronautics and Aeronautics*, Vol. 210, AIAA, Reston, VA, 2005, Chapters 7 and 8.

[2] Mansour, A., Benjamin, M., Straub, D. L., and Richards, G. A., (2001) "Application of Macrolamination Technology to Lean Premix Combustion,"*ASME Journal of Engineering for Gas Turbines and Power*, October 2001, Vol 123, pp796-802.

[3] Straub, D. L., Richards, G. A., Baumann, W. T., and Saunders, W. R., "Measurement of Dynamics Flame Response in a Lean Premixed Single-Can Combustor," ASME Paper 2001-GT-0038, 2001.

[4] Lieuwen, T., "Online Combustor Stability Margin Assessment Using Dynamic Pressure Data," *J. of Engineering For Gas Turbines and Power,* Vol. 127, July 2005, pp. 478-482

[5] Hibshman, J. R., Cohen, J. M., Banaszuk, A., Anderson, T. J., and Alholm, H. A., "Active Control of Combustion Instability In A Liquid-Fueled Sector Combustor," ASME Paper 99-GT-215, 1999.

[6] Nair, S., Rajaram, R., Meyers, A., Lieuwen, T., Tozzi, L., and Benson, K., "Acoustic and Ion Sensing of Lean Blowout in an Aircraft Combustor Simulator," 43rd AIAA Aerospace Sciences Meeting and Exhibit, Reno, NV, AIAA Paper 2005-0932, 2005

[7] Straub, D., Bedick, C., Sidwell, T., Strakey, P., and Casleton, K., "Flashback Studies In A Lean Premixed Combustor Operating On Hydrogen/Natural Gas Fuel Blends," Presented at the Western States Section of the Combustion Institute Spring 2006 Meeting, Boise, ID, 2006

[8] Stuttaford, P., Martling, V., Green, A., and Lieuwen, T., "Combustion Noise Measurement System For Low Emissions Combustor Performance Optimization and Health Monitoring," ASME Paper GT2003-38255.

[9] Sujith, R., Waldherr, G., and Zinn, B., "An Exact Solution For One-Dimensional Acoustic Fields In Ducts With An Axial Temperature Gradient," *Journal of Sound and Vibration*, V184, No. 3, 1995, pp 389-402.

[10] Munjal, M. L., Acoustics of Ducts and Mufflers—With Application to Exhaust and Ventilation System Design, John Wiley and Sons, 1987.

[11] Ferrara, G., Ferrari, L., and Sonni, G., "Experimental Characterization of a Remoting System For Dynamic Pressure Sensors," ASME Paper GT2005-68733.

[12] Van Ommen, J. R., Schouten, J. C., Vander Stappen, M. L. M., and Van Den Bleek, C. M., "Response Characteristics of Probe-Transducer Systems For Pressure Measurements in Gas-Solid Fluidized Beds: How to Prevent Pitfalls in Dynamic Pressure Measurements," Powder Technology, V106, 1999, pp. 199-218.

[13] Bergh, H., and Tijdeman, "Theoretical and Experimental Results For The Dynamic Response of Pressure Measuring Systems," Report NLR-TRF.238, National Aero- and Astronautical Research Institute, Amsterdam, The Netherlands, 1965.

[14] Mahan, J. R., and Karchmer, A., "Aeroacoustics of Flight Vehicles: Theory and Practice, Vol. 1: Noise Sources -- Combustion and Core Noise," Available from AIAA Technical Library, 1991, pp. 483-517.

[15] Englund, D. R., and Richards, W. B., "The Infinite Line Pressure Probe," Proceedings of the 30th International Instrumentation Symposium, Instrument Society of America, Denver, CO, May 7-10, 1984.

[16] Samuelson, R. D., "Pneumatic Instrumentation Lines and Their Use in Measuring Rocket Nozzle Pressure," Nuclear Engine for Rocket Vehicle Applications (NERVA) Program, Report No. RN-DR-0124, July 1967.

[17] Iberall, Arthur S., "Attenuation of Oscillatory Pressures in Instrument Lines," NBS research Paper RP2115, Vol 45, July 1950

[18] Kinsler, L.E., Frey, A. R., Coppens, A. B., and Sanders, J. V., Fundamental of Acoustics, 3rd Ed., John Wiley and Sons, 1982.

[19] Rodarte, E., Singh, GT., Miller, N. R., and Hrnjak, P., "Sound Attenuation in Tubes Due to Visco-Thermal Effects," *Journal of Sound and Vibration*, V231, (2000), pp. 1221-1242.